THE MANCHESTER ECHELLE SPECTROMETER AT THE SAN PEDRO MÁRTIR OBSERVATORY (MES–SPM)

J. Meaburn

Jodrell Bank Observatory, University of Manchester, UK

and

J. A. López, L. Gutiérrez, F. Quiróz, J. M. Murillo, J. Valdéz, and M. Pedrayez.

Instituto de Astronomía Universidad Nacional Autónoma de México, Ensenada, B. C., México

RESUMEN

Se describe el desempeño de la segunda versión del Manchester Echelle Spectrometer en su uso combinado con el telescopio de 2 m de San Pedro Mártir. Este espectrómetro fue concebido para atacar un intervalo limitado de problemas astrofísicos, i.e., donde se requiere estudiar con alta señal a ruido perfiles de líneas resueltos espacialmente, provenientes de fuentes extendidas y débiles. Como consecuencia, el diseño óptico es simple pero muy eficiente. Adicionalmente, se ha incrementado la eficiencia operacional mediante mejoras recientes (2000) al sistema de control. Finalmente, se presentan algunas comparaciones de desempeño con un Fabry-Perot de barrido como un instrumento competitivo en problemas similares y se enfatiza como estos dos tipos de espectrómetros distintos son complementarios.

ABSTRACT

The performance of the second version of the Manchester Echelle spectrometer is described when combined with the San Pedro Martir, 2.1 m telescope. The simplicity but effectiveness of the optical design is explained as a consequence of the spectrometer's dedication to a narrow range of astrophysical problems i.e., where spatially resolved line profiles are required from faint, extended sources at high signal-to-noise ratios.

The improvement in operational efficiency is demonstrated as a consequence of the recent (2000) upgrade of the control system.

Finally, comparisons are made with the performance of competitive stepped Fabry-Perot interferometers on similar problems. The complementarity of spectrometers of different types is emphasized.

Key Words: **INSTRUMENTATION: SPECTROGRAPHS**

1. INTRODUCTION

The Manchester Echelle Spectrometer (MES: Meaburn et al. 1984; Meaburn & Bryce 1993), whose optical layout is shown in Figure 1, is a very simple spectrometer dedicated to a narrow range of astrophysical problems where it performs better than more generalized designs with similar dimensions. In its primary mode a single order of its echelle grating (nominally $\delta = 63.43°$ with 31.6 grooves mm^{-1}) is isolated by a broad, efficient, three-period (top-hat profile) interference filter, eliminating the need for cross-dispersion. Consequently, its primary use,

at Cassegrain or Ritchey-Chretien (RC) foci, is to obtain spatially-resolved profiles of individual emission lines from *faint* extended sources emitting in the range 3900–9000 Å with a spectral resolving power of $\lambda/\delta\lambda \leq 10^5$.

Several secondary modes are available in practice for their inclusion does not impinge on its primary performance. For instance, a direct image of the field can be obtained by both the insertion of a clear area to replace the slit and of a mirror before the grating. For one thing, precise slit positions against images of extended sources can be obtained using this facility.

f/8 RC focus

SPM telescope

clear area
or
long single slit
or
long multi−slits

in   out

* calib. lamps

wheel

interference
filter

ECHELLE GRATING

$\delta = 64.5^\circ$

31.6 grooves mm^{-1}

CCD
detector

plane mirror

(in or out)

grism
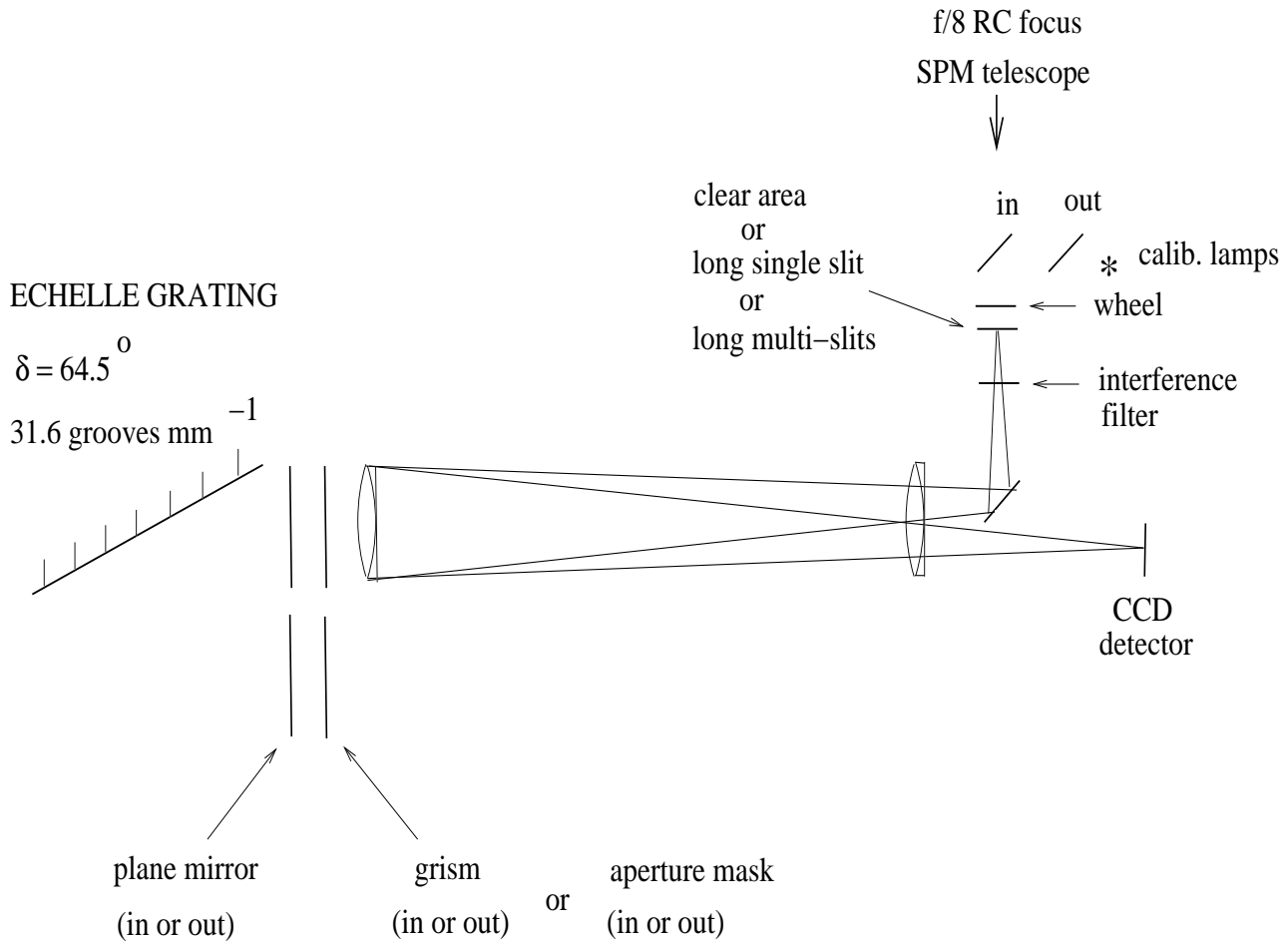
(in or out)

or

aperture mask

(in or out)

Fig. 1. The layout of MES-SPM. All operations are under computer control except the insertion of the grism and aperture mask.

Also, insertion of a grism along with the plane mirror permits longslit, low-dispersion (76.3 Å mm^{-1}) spectra to be obtained.

The first version of MES was commissioned in 1983 on the 3.9 m Anglo-Australian Telescope (AAT) and a second version in 1986 and 1987, respectively on the 2.5 m Isaac Newton Telescope (INT) and 4.2 m William Herschel Telescope (WHT). This second, and more mechanically refined version of MES, was then brought in 1995 for use on the San Pedro Mártir 2.1 m telescope. The obvious attraction of SPM is of course the superb observing conditions (often superior to La Palma, which can be affected by Saharan dust) but also the f/8 Ritchey-Chretien focus matches the f/8 acceptance beam of MES (converting optics had to be included for use on the INT and WHT but not the AAT).

A further, more philosophical, point should be made in this era of 8–10 m diameter telescopes.

There are many topical astrophysical problems associated with very extended, very faint, emission line nebulae, both within the Galaxy or nearby galaxies, that require very long integrations at modest angular resolution (many arcsec) but with long slit lengths projected on the sky. For their investigation there can often be no advantage in using the giant telescopes if the smaller ones are equipped with efficient spectrometers such as MES (or even similar spectrometers with much larger beam diameters but fibre coupled to small telescopes). In fact, sound arguments can be made along these lines for combining MES at the Ritchey-Chretien focus of an even smaller diameter telescope (say 0.5 m) of high optical and mechanical quality. This point is best illustrated by considering the potential observations at 10 km s^{-1} spectral resolution of the many tens of degrees long galactic emission line features at high Galactic latitudes (e.g., Boumis et al. 2001) or the

several degree diameter supergiant shells (and inter-shell) regions of the Large and Small Magellanic clouds (Meaburn 1980) to mention but a few examples of relatively unexplored topical phenomena which can be spectrally featureless on scales even up to 0.5 arcmin. With MES on a 0.5 m diameter telescope the maximum slit length could be 52 arcmin and width ≈ 8 arcsec. It would be wasteful (scientifically and financially) observing these phenomena with a giant telescope even when equipped with a spectrometer with a much bigger beam diameter.

These assertions are consistent with the analysis by Gopal-Krishna & Barve (1999), and reported in Trimble & Aschwanden (2000) of the papers in Nature presenting optical or near-IR results. Twenty-three of the fifty-one such papers came from telescopes of 2.5 m diameter or less.

In the present paper, the performance of MES combined with the SPM 2.1 m telescope is analyzed and the range of astrophysical problems to which it can be applied, competitively, is illustrated by recent examples of its use. Furthermore, the computerized enhancement of the spectrometer's control system (in 2000), which has led to considerably improved operational efficiency, will be explained.

2. DESIGN PRINCIPLES

Why use a high-order reflection echelle grating (with high blaze angle, δ) rather than a low order reflection diffraction grating in the spectrometer for this primary astrophysical objective, i.e., obtaining spatially resolved profiles of a single emission line from an extensive, faint source? To answer this question first consider that for any (single slit) grating spectrometer working on such a problem the product (related to the 'luminosité resolution product' of Jacquinot 1954)

$$\text{merit} = \epsilon \times R \times \delta\alpha \times A \times \ell,\qquad(1)$$

should be maximized to obtain the greatest number of photons in a fixed integration time in each spatial and spectral element, where ϵ is the optical efficiency of the whole system (excluding the telescope), R is the spectral resolving power $(\lambda/\delta\lambda)$ as determined by the angular slit width $\delta\alpha$ to the grating, A is the *exploited* pupil area on the grating and ℓ the angular slit length with respect to the grating. For the actual pupil area, A_0 (see Figure 2)

$$A = A_0(1 - \tan\delta\,\tan\phi)\,,\qquad(2)$$

due to groove masking when $\phi = \phi'$ and $\delta = \delta'$ (see Fig. 2) and when the complications of diffraction
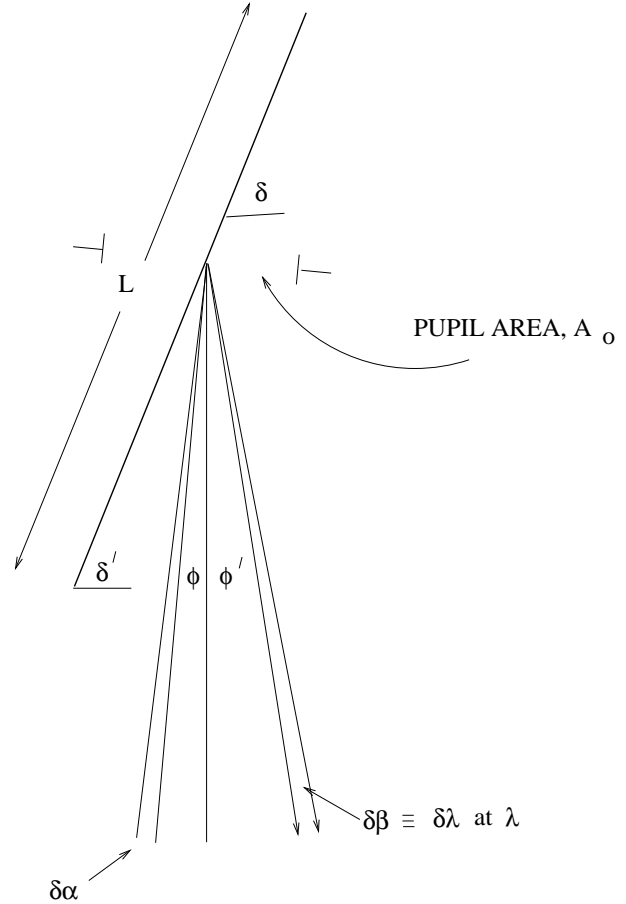

Fig. 2. A schematic diagram of the incident and diffracted light off an echelle grating. A_0 is the exit pupil.

effects at the groove edges are ignored (Schroeder & Hilliard 1980). In other words, A/A_0 in Eq. 2 represents the fractional decrease of the effective area of the grating due to the partial shadowing of the reflecting area of each grating groove by the height of an adjacent groove (groove masking) when the whole grating is illuminated with parallel light, but off-axis by the angle ϕ in Fig. 2.

It is shown in Schroeder & Hilliard (1980) (and see Meaburn & Bryce 1993) that the increase of $R \times \delta\alpha$ with increasing ϕ (Eq. 2) is exactly offset by the consequent decrease in A due to groove masking. However, MES is used in a quasi Littrow mode with $\phi = 1.65°$ which for the present purposes approximates to zero. In these circumstances,

$$R \times \delta\alpha \approx R \times \delta\beta \approx 2\tan\delta\qquad(3)$$

therefore,

$$R \times \delta\alpha \times A = 2A_0\tan\delta\qquad(4)$$

in Eq. 1. In other words, the 'merit' of the spectrometer on this narrow range of astrophysical problems,

for a fixed A, is an increasing function of δ. Consequently, the Bausch & Lomb echelle grating with a measured $\delta = 64.54°$ (nominally $63.43°$) was chosen as the optimum. The Bausch & Lomb grating with $\delta = 76°$ was also an option but requires a grating length of $L = 41$ cm (Fig. 2) to accept the MES 100 mm diameter exit pupil.

3. MES ON THE SPM TELESCOPE

The details of the optical layout of MES (Fig. 1) are given in Meaburn et al. (1984) and only considerations pertinent to its use at SPM will be emphasized here. The light is focused by the telescope on to Chromium deposited slits sandwiched between two sheets of glass anti-reflected on their air/glass outer surfaces. An 800 mm focal length lens acts both as the collimator and camera. This lens firstly directs parallel light on to the 31.6 groove mm^{-1} echelle grating in the 100 mm diameter pupil of the telescope/spectrometer combination. A three-period (flat top) interference filter isolates a particular echelle order. The dispersed echelle spectrum is then focussed by the same lens on to the CCD detector. The SPM telescope focal length is 15824 mm; therefore, with the working aperture of ≈ 2000 mm, the output f/ratio of the telescope matches closely the f/8 acceptance ratio of MES.

3.1. Performance Parameters

The four air/glass surfaces of the single collimator/camera lens (i.e., two cemented doublets) of MES, similarly to those of the slit sandwiches, are coated with three-layer anti-reflection coatings to give ≤ 0.5 percent reflection per surface between 3900–7500 Å Towards longer wavelengths this reflection reverts back to the uncoated value of 4 percent per air/glass surface. Below 3900 Å the coatings become strong reflectors and in any case the flint glass starts to absorb: MES is not useful in this range. The overall efficiency of the spectrometer, without considering the quantum efficiency of the CCD, at the peak of the blaze and with a freshly coated 45° flat is $\epsilon = 32$ percent (from Eq. 1). The operational precautions required to achieve as near as possible to this peak value, and the possible pitfalls when measuring it using standard stars, are described in § 3.2.

Details of the performance of MES on the SPM 2.1 m telescope with existing components are listed in Table 1. In practise, the three available 'slit' holders are used with one clear for imaging and two loaded with any two of the listed slits. Multi-slits are converted to single slits by manually inserted 'dekkars' prior to observing. The usable slit lengths
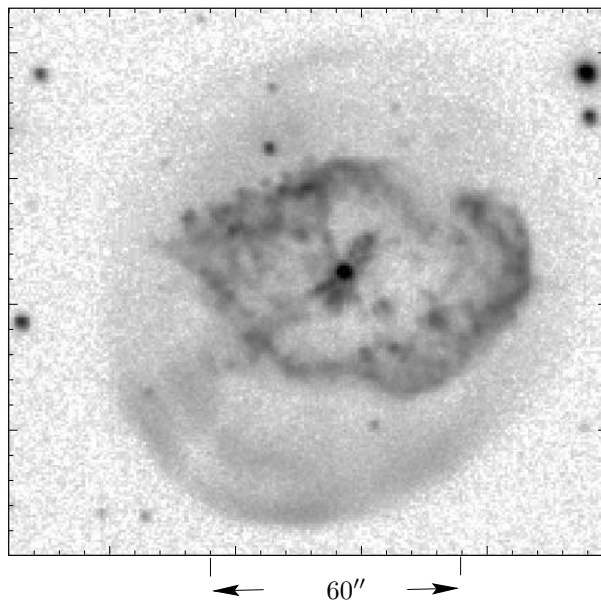

Fig. 3. An image of the hydrogen deficient PN Abell 78 in the light of [O III] 5007 Å taken with MES-SPM. The image of the slit would be a dark line in this representation when superimposed on the image of the nebula.

are limited by the size of the CCD. Simple optical modifications (e.g., insertion of a longer 45° reflecting mirror—see Fig. 1) could double the slit lengths listed in Table 1 as bigger CCDs become available, although at the expense of restricting the slit holder to a two-port system. Four order-isolating interference filters can be loaded at any given time. Samples are listed in Table 1.

A grism can be inserted (see Ivison, Bode, & Meaburn 1994 for a good application), with the plane mirror also in the beam, to give a quick-look 76.3 Å mm^{-1} low-dispersion, second order, long-slit spectrum from ≈ 4500 Å to 6750 Å. Another auxiliary mode (not listed in Table 1) permits approximate spectropolarimetry and imaging polarimetry on bright sources which have linear polarisations ≥ 10 percent. For this, three polaroids are in the above-slit, five-port, wheel (Fig. 1) with orientations with respect to the slit length of 0, 60, and 120 degrees, respectively. One other port in this wheel contains a red-cutter (≥ 7000 Å) for any red side-bands of the below-slit interference filters, and the fifth is clear.

3.2. Efficiency

The primary advantage of this dedicated design is that the optical efficiency of the spectrometer, ϵ in Eq. 1, is high as a consequence of the minimum number of optical components (e.g., no cross-dispersion)

TABLE 1

PARAMETERS ON THE SPM 2.1 M F/8 TELESCOPE (F.L. = 15824 MM)

ECHELLE SPECTROMETER			
slit widths (μm) (km s^{-1}) (arcsec)	**option 1** 70 $\equiv 5$ $\equiv 0.9$	**option 2** 150 $\equiv 10$ $\equiv 2.0$	**option 3** 300 $\equiv 20$ $\equiv 3.9$
multi-slits	**number of slits** 10 slits 5 slits 3 slits	**free spectral range** 1.65 mm separation $\equiv 138$ km s^{-1} 3.3 mm separation $\equiv 277$ km s^{-1} 6.6 mm separation $\equiv 555$ km s^{-1}	**separation on sky** $\equiv 21.5$ arcsec $\equiv 43$ arcsec $\equiv 86$ arcsec
slit length	**linear** 30 mm 60 mm	**on sky** $\equiv 6.5$ arcmin $\equiv 13$ arcmin	**comments** current max. not yet implemented
order isolator filters	**center (bandwidth)** 6730 (100) Å	**center (bandwidth)** 6580 (100) Å	**center (bandwidth)** 5020 (70) Å
echelle grating	**blaze angle** 64.5 deg.	**grooves mm^{-1}** 31.6	**ruled area** 128 x 254 mm^2
GRISM SPECTROMETER			
	dispersion 76.3 Å mm^{-1}	**spectral range** 4500 – 6750 Å	
IMAGING			
field area (max)	**linear** 25 x 30 mm	**on sky** $\equiv 5.4$ x 6.5 arcmin^2	

and use of transmission optics to minimise ageing losses.

The first operational precaution to ensure that this is achieved in practise is to place the exit pupil of the telescope on to the entrance pupil of the spectrometer (at the echelle grating). After each re-installation on the telescope the grating housing needs to be removed and the daylight-illuminated image of the telescope primary mirror, adjusted by tilting and turning (with two rotating screws) the 45° mirror in Fig. 1, until it is centred on the doublet collimator/camera lens nearest the grating. This can be achieved to high degree of accuracy by eye.

The correct order of the echelle spectrum for a particular isolating filter (see Table 1) must also be checked prior to each observing run. Adjacent orders

to the optimum, at very low efficiency (say ≤ 10 percent) can easily be selected by incorrect rotation of the echelle grating by even a few degrees. This is trivial to check before an observing run by taking a sequence of white light spectra of a Tungsten lamp for a range of grating angles with any order-isolation filter (see Table 1) in place. Once the correct angle is established it is true for the whole wavelength range.

After these elementary precautions had been taken many confirmations of $\epsilon \approx 30$ percent have been made for MES prior to use on the SPM telescope by taking the spectra of standard stars. There are a surprisingly large number of pitfalls in this process for (1) the absolute spectrum of the star must be known over the relatively small wavelength range of MES (such standard spectra are often de-

rived from measurements through very broad filters), (2) this standard spectrum must be converted into photons/s/unit area/unit wavelength range over the wavelength range being considered and for the top of the atmosphere, (3) the atmospheric absorption, ABS, on the night in question (units of magnitude/air-mass) and at the wavelength used must be known, (4) the intensity reflection coefficients, r, of the primary and secondary mirrors must be known, as should (5) the quantum efficiency of the detector, Q, and the conversion ratio, X, of detection counts for the CCD to photon generated electrons (electrons/ADU). It is then essential to take a slitless spectrum of the standard star to prevent slit centring losses.

A particularly sound measurement comes from a slitless spectral observation in June 1998 with MES on the SPM-2.1 telescope of the standard star Feige 56 ($M_V = 11.34$) with $air - mass = 1.445$ at the peak of the blaze at 6550 Å and where all of these tuning precautions had been taken. For ABS = 0.2 mag/airmass and for the Tek1 CCD parameters given at the time of $Q = 0.65$ and $X = 1.22$, then this measured value of overall efficiency $\epsilon \times r^2 = 23\%$ therefore, assuming $r = 0.9$, $\epsilon = 28\%$. Here, the overall efficiency has been defined as the number of stellar photons incident on the CCD (in each 0.1 Å channel and 295 integration time) divided by the photons collected by the telescope in the same wavelength range and time. The collecting area, corrected for the obstruction of the housing around the Ritchey-Chretien secondary mirror, was estimated as 2.97×10^4 cm^2.

The uncertainty in these absolute efficiency measurements is dominated by the uncertainty in knowledge of ABS, X, Q, and r but reasonably substantiates the $\epsilon \approx 30\%$ predicted performance of MES-SPM. However, this measurement, along with the presentation of the parameters used in the calculation, ensures that future users with different CCDs can check the current performance and tuning of the whole system (telescope, CCD plus MES-SPM).

3.3. *Sky Plus Slit Imaging*

One considerable advantage of this design is the ability to image the (max. 5.4×6.5 arcmin^2) field being observed spectrally. With a 1024×1024 (24 μm) pixels CCD this field is restricted to 5.12×5.12 arcmin^2 (and the echelle slit length to 5.12 arcmin). This is achieved by driving the plain mirror in Fig. 1 into the beam with the slit area clear. Furthermore, a sky-illuminated image of the slit can be superimposed on to this image if desired. This is

achieved by taking an image of the target with the 'clear area' in place and the 'plane mirror-in' (see Fig. 1), followed by a similar image but with one of the slit options in place. The centering of the slit on a small, isolated target (e.g., an extra-galactic PN) is facilitated by this provision though note that it is best to take the spectrum after the slit image in case of minor positional errors in the direction perpendicular to the slit length.

An example of this imagery is shown in Figure 3.

3.4. *Ghosts and Occulting Strips*

Every optical system has unwanted 'ghosts'. Here the primary ghost is a consequence of the nearly flat outer surfaces of the component of the camera/collimator lens nearest the echelle grating in Fig. 1. This ghost manifests itself as an out-of-focus, displaced, image of the slit produced by ≤ 0.5 percent of all the light passing through the slit and echelle order-sorting filter. Once recognised it has caused little confusion over many observations.

A plethora of far fainter ghosts of course exist and can be seen by illuminating the slit with a bright star. In the investigation of faint sources these cause few problems. However, when observing faint circumstellar nebulae around bright stars (say 4.8 mag like P Cygni) a Chromium occulting strip, a few arcsec wide, can be placed (manually) in front of the slit to eliminate the contaminating continuum as far up the optical chain (towards the telescope) as possible. This also represents an advantage of the current design where the slit area is so readily accessible.

3.5. *Aperture Masks*

The emphasis here has been so far on observations of faint line emission sources which is the primary application of this spectrometer. However, occasionally, the line profiles of bright sources are needed. In these circumstances there is an abundance of light and angular resolution is at a premium. It can then be desirable to cut the telescope aperture down to a quarter by insertion near the exit pupil of an aperture mask with an offset hole (in the grism slot—see Fig. 1). Restricting the aperture alone improves the 'seeing' (wavefront tilt effects) somewhat. The offsetting of this hole is to place it between the images of the RC secondary holders and the central obstructed area in the pupil. Diffraction spikes are then nearly eliminated. A further advantage is that the change from f/8 to f/16 in the optical chain improves the depth of the field for both the telescope and spectrometer and makes focussing less critical. The achieved resolution in sample observations has
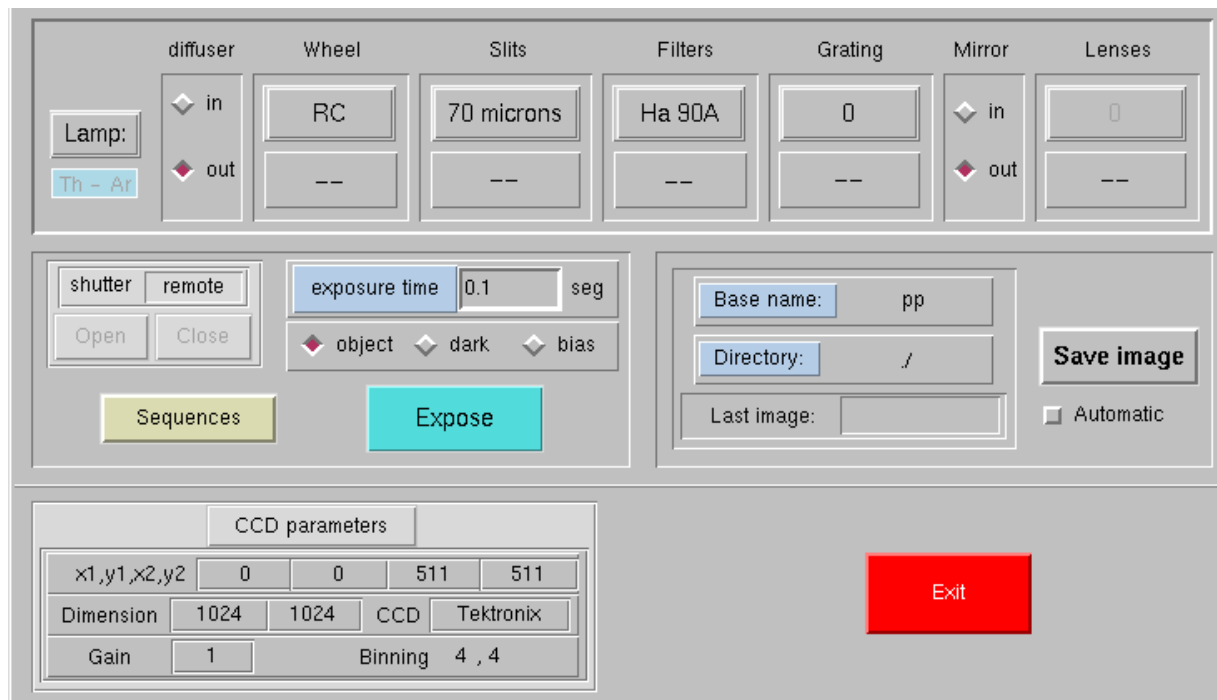
Fig. 4. The control panel of MES-SPM and the CCD. 'Wheel' is for the position of an auxiliary above-slit filter wheel containing a red-cutter (RC), polaroids and a clear area. 'Grating' indicates rotation of the echelle grating and 'Lenses' the focussing position of the compound collimator/camera lens.

been improved from ≈ 1 arcsec to ≈ 0.7 arcsec by using this device i.e., that is an improvement by a factor two in the area of a resolved element in an image, and a factor of 1.4 along a longslit spectrum.

4. CONTROL SYSTEM

Most of the spectrometer functions, and operation of the CCD, have now been brought under the control of a single PC. The observer is faced with the state-of-system display shown in Figure 4 and many of the common sequences of operations are initiated by single commands.

This is best illustrated by the most common sequence an observer will require with MES operating in its primary mode i.e., long single or multi-slit observation of the profiles of a faint extensive source. After compiling the requirements a single command will drive the required slits and filter into position, adjust the orientation of the echelle grating and focus position of the camera/collimator lens. The CCD shutter will then be opened and the integration on the source made for a pre-specified number of seconds. On completion, the Th/Ar arc lamp

will be switched on, its reflector driven in front of the beam. An arc spectrum will then be taken for a pre-determined integration time. The lamp will be switched off and the arc reflector removed. The plane-mirror will then be driven into place near the pupil (see Fig. 1) and a sky-illuminated image of the slit taken. The clear slit area will be driven in and an image of the source taken. The system will then revert back to its starting configuration ready for the next sequence i.e., long slit in place and plane mirror out.

In this way, a long slit echelle spectrum of the source is obtained followed by the calibration arc spectrum and an image of the slit against that of the source.

5. DISCUSSION

Here, examples of successful observations on topical problems using MES will be illustrated, and a comparison made with a competitive Fabry-Perot spectrometer.
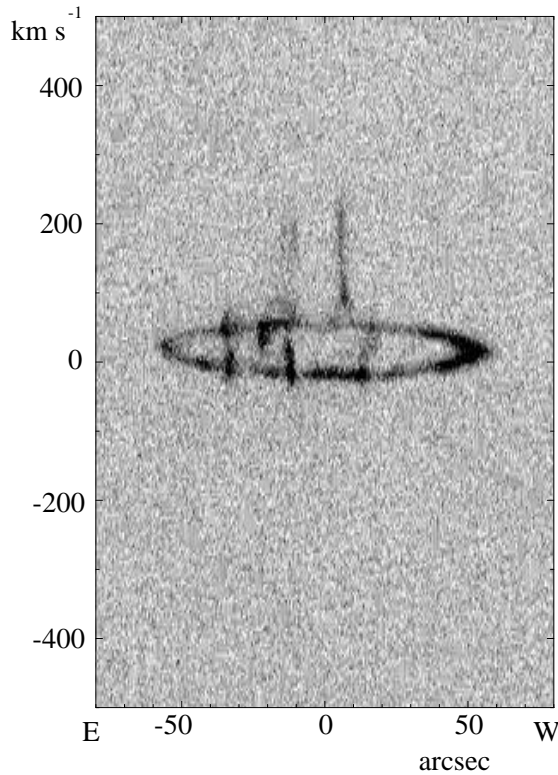
Fig. 5. A grey scale representation of the longslit pv array of [O III] 5007 Å line profiles across the hydrogen deficient PN Abell 30. The velocity 'ellipse' illustrates the radial expansion of the outer shell whereas the velocity 'spikes' show the presence of wind-driven high-speed flows.

5.1. *Examples of Use*

The performance of MES–SPM in its primary mode can best be illustrated by examples of its application on topical problems.

Highly collimated velocity spikes (Figure 5) were discovered (Meaburn & López 1996) in the position-velocity (pv) array of [O III] 5007 Å line profiles from the core of the hydrogen deficient PN Abell 30. High-speed outflows were found (López et al. 1998) in the pv arrays of Hα profiles over the extra-ordinary giant lobes of KjPn 8 (Figure 6).

Multi-slit observations (Meaburn et al. 1998) of the [N II] λ6584 Å line profiles of the cometary knots of the Helix nebula are shown in Figure 7.

Finally, the [N II] λ6584 Å line profiles over the poly-polar lobes of NGC 2440 are shown in Figure 8 (López et al. 1998).

5.2. *Comparisons*

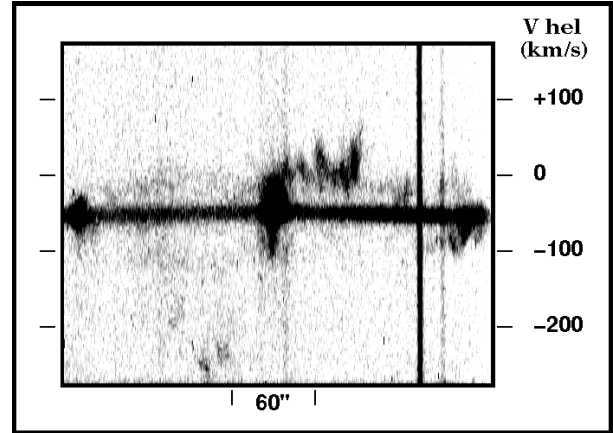Every dedicated spectrometric device should have a niche in which it out-performs competitive

Fig. 6. A pv array of [N II] λ6584 Å line profiles over the lobes of the extra-ordinary bi-polar PN KJPn 8. Many faint high-speed features are present.

systems. Furthermore, it should be realized that different types of spectrometer invariably produce complementary information on a source if they all detect its emission. A comparison must be made between the performance of MES and a stepped Fabry-Perot (SFP) working on faint line emission sources, for there are often misunderstandings about the performance of the latter. These arise simply because an FP interferometer sends an overwhelming fraction

$$F = (N_e - 1)/N_e \,, \tag{5}$$

of the incident monochromatic light back to the sky. Here, N_e is the effective 'finesse' i.e., by Gaussian approximation

$$N_e^{-2} = N_r^{-2} + N_d^{-2} \,, \tag{6}$$

and N_r and N_d are the reflection and defect finesses respectively. N_d limits practical FPs to around 50 mm diameter to give $N_e \approx 25$, therefore $F \approx 0.96$ i.e., only 4 percent of the incident light is transmitted. A simple realization of this massive loss is to look at an FP fringe pattern of a monochromatic source in reflection. The FP fringes are now narrow dark bands on a bright background. In fairness it should be noted that MES could be considered very efficient spectrally but very inefficient spatially.

A comparison will be made between MES with $A_0 = A_{MES}$ for a 10 cm pupil width and the SFP with $A_0 = A_{SFP}$ for a 50 mm diameter. Echelle gratings can be ≥ 25 cm in width but for use at the Ritchey-Chretien/Cassegrain foci of medium-sized telescopes this width is restricted, for mechanical reasons, to ≈ 10 cm as in MES. Similarly this comparison is best made with typical MES
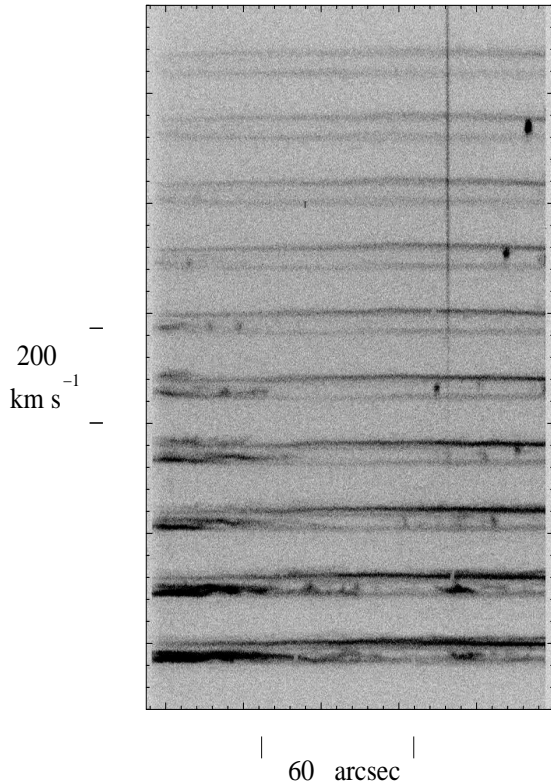
200
km s^{-1}

| 60   arcsec |

Fig. 7. A pv array of [N II] λ6584 Å line profiles of the Helix planetary nebula obtained with a 10-element multi-slit. The profiles of the cometary knots are between the extensive split profiles from the expanding host nebula.

and SFP parameters. Consider MES with a single long slit $f\delta\alpha = 150$ μm wide (where f is the camera/collimator focal length) to give $f\delta\beta = 2 \times \delta x$ where δx is the size of a data taking window on the CCD. In these circumstances the spectral resolution $\delta\lambda \equiv$ 10 km s^{-1} and inter-order separation $\Delta\lambda \equiv 2631$ km s^{-1}. The comparable FP for $\delta\lambda \equiv 10$ km s^{-1} and $N_e = 25$ then has the very much smaller $\Delta\lambda \equiv 250$ km s^{-1} which itself is an independent disadvantage because of the ambiguities that can arise when extensive Doppler broadened line profiles are being investigated. However, if a ten element MES multislit is used (see Table 1) the free spectral range is down to that of the comparable SFP.

A good way of appreciating the behavior of the SFP is to consider the signal received by each 2×2 box of data taking windows (one spatial element) on the CCD, where the box width of $2 \times \delta x$ matches the SFP fringe width at the edge of a circular field. The SFP must be scanned in wavelength *sequen-*
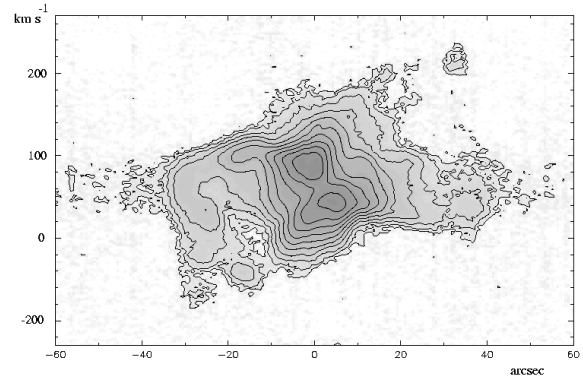

Fig. 8. A pv array of [N II] λ6584 Å line profiles over the poly-polar lobes of the PN NGC 2440.

tially, with $2 \times N_e$ steps through $\Delta\lambda$. The signal, however, is received simultaneously in all spatial elements over its wide field to generate the 'data cube' of line profiles. On the other hand, MES obtains the signal in all its spectral elements *simultaneously* but now only for those spatial elements along its long $f\delta\alpha$ wide slit.

Quantitatively significant comparisons of performance can now be made which are heavily dependent on the nature of the information that is being sought. If interest is in obtaining line profiles at the highest signal to noise ratio (SNR in photon noise limited conditions) from a faint source intercepted by only those spatial elements (say $2 \times \delta x$ long) that are along the length of a MES slit then the number of photons received in a given integration time is $2 \times N_e \times A_{\mathrm{MES}}/A_{\mathrm{SFP}}$ greater for MES than SFP i.e., 200 times greater. Put another way: to get the same SNR in these circumstances for all spatial elements in the whole SFP field (assuming the source filled this larger area) would require 200 times the MES integration time. As many of the integration times employed with MES on topical faint line emission sources are ≈ 1 hr then a 200 hr integration would be required with SFP to be competitive in this specific but very common application. This would be the case when searching for the very faintest, high-velocity components in the profiles of an emission line from an extensive gaseous nebula of whatever type. The values of the optical efficiencies (ϵ in Eq. 1 for MES) are assumed to be similar for MES and SFP.

Where the SFP starts to win over MES is if line profiles are required for every $2 \times \delta x$ wide spatial element over the whole of the extensive SFP field

that is $\approx (fx\ell)^2$ in area. The aim would be to map two-dimensionally the profiles of an emission line.

The single slit MES must now be stepped across the source, sequentially (i.e., with $\ell/(2 \times \delta x)$ steps equal to several hundred) to cover the whole field. This handicap is partially mitigated (up to 10 times—see Fig. 7) if multi-slits are used (with a consequent restriction in $\Delta\lambda$ to ≈ 138 km s^{-1}). For a good example of where this advantage of an SFP has been exploited in practice see Rosado et al. (2001), though note that the observations were of the core of M 42 which is very bright. Incidentally, similar comparisons apply to a conventional grating spectrometer with an intermediate resolution SFP.

Fibre-optic format changers (now often referred to as integral field devices) reverse the situation dramatically in favor of MES over a circular field whose size is the projected area of the fibre bundle on the sky. For instance, 169 fibres in a circular bundle have been used (Meaburn, Christopoulou, & Goudis 1992) to feed 3 parallel slits of MES on the 4.2 m William Herschel telescope. Within this field diameter then MES beats SFP by ≤ 200 times (this gain is decreased from 200 by fibre packing fractions and additional optical inefficiencies). This led to the development being called MATADOR at the time (versus Taurus the UK SFP—see the report in Clayton 1989). This fibre optic, format changing, option has not yet been implemented on MES-SPM.

The complementarity of spectrometers must be re-emphasized. For instance, an SFP could be used to identify the whereabouts of high-speed line emission phenomena in a wide field (e.g., PNe in a Local Group galaxy, HH-objects in an extensive Galactic [N II] 6583 Å region etc.) followed-up by MES observations of specific targets to obtain line profiles at the highest SNR.

5.3. *Developments*

Several developments to the existing instrument suggest themselves. The most easily achieved is installing the longer (13 arcmin) slit. The instrument has the optical capacity to accept this increased slit length without vignetting. A longer rectangular $45°$ mirror in Fig. 1 is required as is either 3/1 condensing optics feeding an existing 1024×1024 ($24\mu m$) pixel CCD or a larger CCD (mosaiced?) if one became available.

The factor of merit (Eq. 1) could be immediately doubled if an echelle grating with $\delta = 76°$ were installed. This grating though would have to have a length of 41 cm and is not commercially available, but two could be possibly mosaiced.

The provision of a fully micro lensed fibre-optic format changer would dramatically enhance the performance for sources the size of the circular input fibre bundle. These devices are manufactured only in specialised groups and are currently expensive.

The same version of MES, when at La Palma, has been used (e.g., Bryce et al. 1992) with 30 μm wide slits to give 3 km s^{-1} resolution when combined with the Image Photon Counting System (IPCS—Boksenberg & Burgess 1973) with 15 μm wide data taking windows. A similar resolution could be achieved with a CCD with pixels of this size.

A minor improvement would be to replace the $45°$ flat in Fig. 1 with a prism, with three-period anti-reflection coatings on its surfaces perpendicular to the optical axis and with a sealed reflection coating on its hypotenuse face. This would have a very high 'reflectivity' as well as negligible degradation with age. Also, a light clamp operating on the slit tray, perpendicular to the slit length, and driven into place after each slit movement, would improve the positional reproducibilty of the slit.

REFERENCES

Boksenberg, A., & Burgess, D. E. 1973, Proc. Symp. on TV Type Sensors, p. 21, eds. J. W. Glaspey & G. A. H. Walker, held in the University of British Columbia

Boumis, P., Dickinson, C., Meaburn, J., Goudis, C. D., Christopoulou, P. E., López, J. A., Bryce, M., & Redman, M. P. 2001, MNRAS, 320, 61

Bryce, M., Meaburn, J., Walsh, J. R., & Clegg, R. E. S. 1992, MNRAS, 254, 477

Clayton, C. A. 1989, A&A, 213, 502

Gopal-Krishna & Barve, S. 1999, Bull. Astron. Soc. India, 26, 417

Jacquinot, P. J. 1954, Opt. Soc. Amer., 44, 761

Ivison, R. J., Bode, M. F., & Meaburn, J. 1994, A&AS, 103, 2011

López, J. A., Meaburn, J., Bryce, M., & Holloway, A. J. 1998, ApJ, 493, 803

López, J. A., Meaburn, J., Bryce, M., & Rodríguez, L. F. 1997, ApJ, 475, 705

Meaburn, J. 1980, MNRAS, 254, 477

Meaburn, J., Blundell, B., Carling, R., Gregory, D. E., Keir, D. F., & Wynne, C. G. 1984, MNRAS, 210, 463

Meaburn, J., & Bryce, M. 1993, Optics in Astronomy, 32nd Herstmonceux Conference, p. 9

Meaburn, J., Clayton, C. A., Bryce, M., Walsh, J. R., Holloway, A. J., & Steffen, W. 1998, MNRAS, 294, 61

Meaburn, J., Christopoulou, P. E., & Goudis, C. D. 1992, MNRAS, 256, 97

Meaburn, J., & López J. A. 1996, ApJ, 472, L45

Rosado, M., de la Fuente, E., Arias, L., Raga, A., & le Coarer, E., 2001, ApJ, 122, 1928

Schroeder, D. J., & Hilliard, R. L. 1980, App. Opt., 19, 2833

Trimble, V., & Aschwanden, M. J. 2000, PASP, 112, 434

Leonel Gutiérrez, J. Alberto López, J. M. Murillo, M. Pedrayes, F. Quiróz, and J. Valdéz: Instituto de Astronomía, UNAM, Apdo. Postal 877, 22860 Ensenada, B. C., México (jal@astrosen.unam.mx).

John Meaburn: Jodrell Bank Observatory, University of Manchester, Macclesfield, Cheshire, SK11 9DL, UK (jm@ast.man.ac.uk).